Using a syntonized Free Fall Grid of atomic clocks in Ehlers-Pirani-Schild Weyl space to derive second order in Φ/c^2 relativistic GNSS redshift terms

E.P.J. de Haas[1, a)]

Nijmegen, The Netherlands

(Dated: October 17, 2017)

In GNSS, the improvement of atomic clocks will lead to Φ/c^2 in relativistic gravitational redshift three to four decades from today. Research towards a relativistic positioning system capable of handling this expected accuracy is all based upon the Schwarzschild metric as a replacement of todays GNSS Euclidian-Newtonian metric. The method employed in this paper to determining frequency shifts between atomic clocks is an intermediate Minkowski-EEP approach. This approach is based on relating two atomic clocks to one another through a background ensemble of frequency gauged clocks, a grid. The crucial grid of this paper, the Free Fall Grid or FFG, can be related to the Ehlers-Pirani-Schild P-CP Weyl space formalism, when applied to a central mass. The FFG second order in Φ/c^2 redshifts are derived for static to static, static to satellite and satellite to satellite atomic oscillators and then compared to GR-Schwarzschild and PPN (Parametrized Post Newtonian) results.

---

a)Electronic mail: haas2u@gmail.com

CONTENTS

I. INTRODUCTION

In this paper, the second order in Φ/c^2 gravitational relativistic redshift accuracy is the topic. In GNSS and geodesy terms, that means a tenth of a millimeter location accuracy. This accuracy, determined by the improvement of atomic clocks, will be the inevitable future of GNSS some three to four decades from today. Research towards a relativistic positioning system capable of handling this expected accuracy is all based upon the Schwarzschild metric as a replacement of todays Euclidian-Newtonian metric.

The method employed in this paper to determining frequency shifts between identical clocks is a Minkowski- EEP (Einstein Equivalence Principle) approach, thus an intermediate step in between todays Euclidian-Newtonian GNSS 1.0 and tomorrows GR-Schwarzschild GNSS 2.0. This hypothetical GNSS 1.5 approach is based on relating two atomic clocks to one another, clocks in different states of motion and at different locations in a central field of gravity, through a background ensemble of frequency gauged clocks, a grid.

The crucial grid of this paper, the Free Fall Grid, will be constructed and justified in several steps, starting with an Euclidian rectangular lattice of syntonized static clocks in free space. An Euclidian radial lattice will be a step towards a radial lattice of static clocks around a central mass, a lattice that fundamentally lacks syntonization. From there, the Einstein Equivalence Principle will lead to the Free Fall Grid. This Free Fall Grid can be related to the Ehlers-Pirani-Schild P-CP Weyl space formalism, when applied to a central mass.

The Free Fall Grid will lead to the connection between two static clocks which, in first order in Φ/c^2 relative accuracy, will be identical to the exact Schwarzschild redshift result. From there, the Free Fall Grid second order in Φ/c^2 static redshift is calculated and compared to GR-Schwarzschild and PPN (Parametrized Post Newtonian). Derived next are the FFG connections between a satellite and a ground station and then between two orbiting satellites. In the end a FFG extension of the Schwarzschild metric is proposed, mirroring the PPN method. But it all starts with the expected development of ever more accurate atomic clocks.

II.   THE FUTURE OF GNSS: SECOND ORDER IN Φ/c^2 ACCURACY

In GNSS systems, engineers use an Euclidean or Newtonian stationary grid in free space attached to the center of the earth and then apply corrections. These corrections might be due to rotation (Sagnac effect, first order in v/c), velocity (classical Doppler effect, first order in v/c; Special Relativity time dilation, second order in v/c) and gravity (General Relativity time dilation, first order in Φ/c^2, so second order in v_{esc}/c) (Ashby, 2002, 2003; Hećimović, 2013).

Since a few decades, several researchers pointed out that such a Newtonian GNSS system with Einsteinian corrections is rather anachronistic and that it would be more logical to construct an Einsteinian GNSS from the ground up (Kheyfets, 1991; Coll, 2001; Bahder, 2001, 2003; Coll, 2003; Ruggiero et al., 2008; Čadež et al., 2011; Bertolami and Páramos, 2011; Coll, 2013; Pascual-Sánchez et al., 2013; Gomboc et al., 2014; Kostić et al., 2015; Puchades and Sáez, 2015, 2016). In an ESA report, the basic idea is expressed as:

> *A simple way to avoid having to deal with the defects of Newtonian theory is to change the paradigm. Instead of modeling the system in a Newtonian framework and adding relativistic corrections, the positioning system could be modeled directly in general relativity. [...] A local Schwarzschild frame was designed, based on the clock signals originating from four satellites. (ESA, 2010)*

Relativistic positioning systems are designed under the assumption that spacetime has a Schwarzschild metric. This corresponds to an Earth that is isolated, static and spherically symmetric (Puchades and Sáez, 2016). Satellites on time-like geodesics, photons on null geodesics and users on or 'near' the earths geoid are the basic ingredient of such a relativistic GNSS, against the background of the Schwarzschild metric (Kheyfets, 1991; Puchades and Sáez, 2016).

Reading the mentioned research on GR Schwarzschild based GNSS gives the impression that, after the promising first initiatives, progress is somewhat stalled. This might be due to the discrepancy between the complexity of GR-Schwarzschild on the one hand and the technical robustness of todays operating GNSS on the other hand. This robustness seems to be interwoven with the relative simplicity of the Newtonian-Euclidian framework. In this paper I propose to go for an intermediate relativistic framework for GNSS, a Minkowski plus Einstein Equivalent Principle (EEP) approach. In the not to far away future of GNSS,

second order in Φ/c^2 accuracy will be the new normal and in such an environment, corrections to Newton-Euclidian basics will probably not be sufficient any more. Minkowski-EEP relativistic GNSS might be a pragmatic and realizable intermediate towards a fully GR-Schwarzschild GNSS.

My Minskowski-EEP approach has a theoretical background in the form of the Ehlers-Pirani-Schild (EPS) Weyl space analysis and a more practical side in the form of syntonized grids of atomic clocks in Einstein Elevators. Future second order in Φ/c^2 accuracy is driven by an ongoing improvement of atomic clocks, roughly gaining a factor 10 accuracy every decade. This pragmatic version of the EPS Weyl Space approach can be temporarily positioned in between present day Euclidian-Newtonian GNSS 1.0 and a future GR-Schwarzschild GNSS 2.0 because it combines the Minkowski metric with EEP.

The greatest push towards GNSS 2.0 will come from the to be expected improvement in the accuracy of precision clocks as the heart of all GNSS satellites. In Galileo, clocks with a relative accuracy of 10^{-14} are employed. Todays scientific research precision clocks reach a relative accuracy of 10^{-17} and improve by a factor of 10 every decade (Delva and Lodewyck, 2013). Today only first order in ϕ/c^2 relativistic effects, of 10^{-10} relative impact, are taken in account in GNSS 1.0 operational technology, but a future relativistic GNSS 2.0 must be expected to handle second order effects too, with a 10^{-20} relative impact. Accumulative effects in clock drift might even speed up the relevancy of second order in ϕ/c^2 effects for future GNSS practices. In the already mentioned literature on relativistic GNSS there is scarcely any attention for this second order accuracy issue. In (Blanchet, L. et al., 2001), the $1/c^3$ order of accuracy is investigated, while mentioning that the ϕ^2/c^4 accuracy isn't an issue yet because it is in the 10^{-20} relative frequency shift range.

This paper tries to fill the gap by treating these second order effects in an adapted EPS Weyl space environment. The outcomes will be compared with the result reached using the usual Schwarzschild metric and the PPN perturbative expansion of it as presented in (Castel-Branco et al., 2014). The first order effects are identical in both approaches, the second order effects deviate. Given the fact that the Schwarzschild metric is known to be limited to weak fields of gravity, the question rises, how weak is weak when second order in ϕ/c^2 effects are taken into account? Is the Schwarzschild metric up to the task of becoming the backbone of GNSS 2.0?

Fundamental in the approach of this paper, the Free Fall Grid method to handle second

order frequency shift accuracy, is to analyze gravity using relative frequency shifts as one of the basic inputs. Such a method is also looming in today's geodesy, the secondary context relevant for this paper. In modern gravitational geodesy scientists are investigating the relativistic frequency shift as a new observable type for gravity field recovery (Mayrhofer and Pail, 2012). Driven by this development, modern geodesy is about to go through a change from the Newtonian paradigm to Einstein's theory of general relativity (Kopeikin et al., 2017). A new generation of atomic clock is the game changer for this new domain of chronometric geodesy, and requires additional new techniques to be developed in the field of frequency transfer and comparison (Delva and Lodewyck, 2013). The paradigm shift is based on the principle of frequency comparison between two clocks in order to measure the frequency shift between them (Delva and Lodewyck, 2013). The knowledge of the Earth's gravitational field has often been used to predict frequency shifts between distant clocks. In relativistic geodesy, the problem is reversed and the measurement of frequency shifts between distant clocks now provides knowledge of the gravitational field (Delva and Lodewyck, 2013). This reversal also looms in our EPS Weyl based approach.

Second order accuracy in relativistic frequency shift measurement isn't just a too far away future to be concerned about today. In 2010 a research group reported the measurement of the height difference between two atomic clock using the gravitational redshift:*the result of* 37 ± 15 *cm agrees well with the known value of* 33 *cm (Chou et al., 2010)*. Simple calculations show that for an accuracy of 1 *cm*, the measured frequency difference of $\frac{\Delta f}{f} \approx 10^{-18}$ is necessary (Delva and Lodewyck, 2013). Thus a second order in Φ/c^2 accuracy ($\approx 10^{-20}$) implies a height resolution in geodesy of a tenth of a millimeter. The best clocks of today reach relative uncertainties in the $10^{-17} - 10^{-18}$ range. Progress continues rapidly, with no hard limit in sight (Wolf et al., 2017). Todays practical use of General Relativity in geodesy implies an accuracy in gravitational redshift in between first order and second order in Φ/c^2. Research in fundamental theory should prepare for the second order in Φ/c^2 technical accuracy, the 0.1 *mm* range, to be relevant in GNSS 2.0 thirty years from now.

III.   THE EHLERS-PIRANI-SCHILD FORMALISM APPLIED TO A CENTRAL MASS

The Ehlers, Pirani and Schild or EPS formalism will function as a theoretical background for the more pragmatic Free Fall Grid approach towards the GNSS, using Einstein Elevators on frequency gauged grids. In these Einstein Elevators, monitored atomic oscillators are the essential ingredient, not synchronized time keeping clocks. Some of these atomic oscillators will be moving on a geodesic, thus in free fall. Others will be stationary in a central field of gravity.
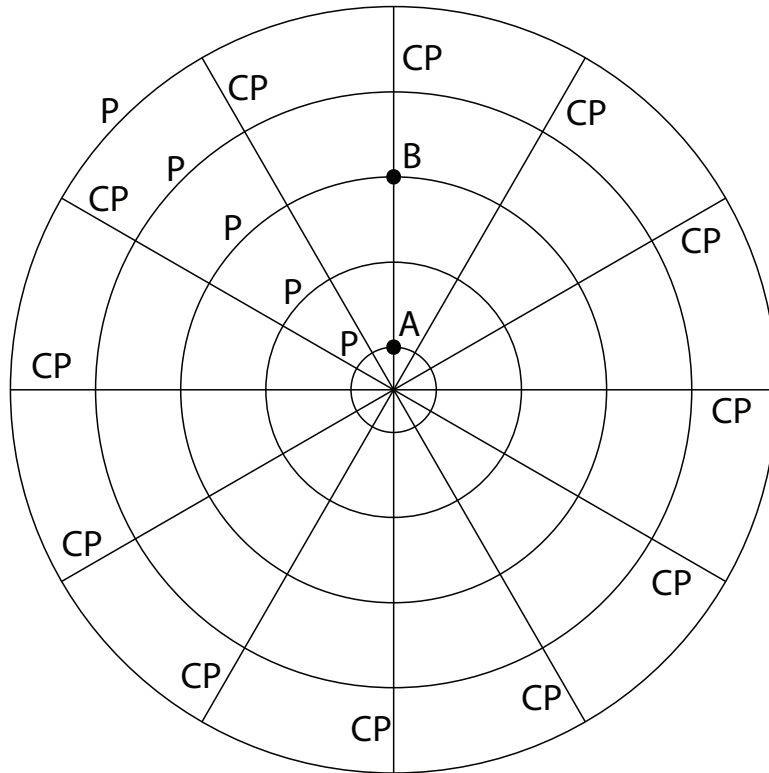

FIG. 1. Ehlers-Pirani-Schild Weyl space, around a central static mass M filling up the smallest circle, with a radial CP structure and a tangential P structure. A and B are static atomic clocks on the P structure but also connected through the CP structure. Photons cannot orbit M on a P geodesic but they can move along a CP geodecis. A and B on different P geodesics and have to communicate through the CP geodesics. GNSS satellites are on a P geodesic, communicating with Earth through CP geodesics.

According to EPS, rigid rulers and standard clocks are not appropriate as fundamental objects for constructing a relativistic space-time geometry. EPS wrote that the choice of Synge for particle and clock as basic concepts was a smart one for deductive purposes, but not for constructive ones. EPS used freely falling particles and light signals for the constructive approach. Light signals are light-like null geodesics and freely falling particles are time-like geodesics of a Lorentzian metric. Standard clocks should then be characterized with the help of light signals and freely falling particles (Ehlers et al., 2012; Perlick, 2016). EPS tried to show how space-time geometry can be constructed from a small number of assumptions/properties about light propagation and free fall (Ehlers et al., 2012).

Freely falling particles move on what is called time-like or P geodesics. A set of such P geodesics form a projective structure (Capozziello et al., 2012). Light propagates on null geodesics or C geodesics and a set of such geodesics forms a conformal structure. CP geodesics are those geodesics that are the paths of both freely falling particles and light signals. Most geodesics are either C or P geodesics. Around a central mass M, as filling up the smallest circle in fig. (1), satellite orbits form P geodesics and the radial lines are CP geodesics. A light ray that is not directed to or from the center of M will follow a bended hyperbolic path around M. Freely falling particles can never track a light ray on such a path. Light rays in turn cannot orbit M. But the radial lines are both C as P geodesics, thus CP geodesics. A manifold with a CP structure is what EPS called a Weyl Space (Ehlers et al., 2012). According to (Ehlers et al., 2012), with some additional assumptions, every Weyl space also was a Riemann space.

One of the basic characteristics of a CP geodesic is that a freely falling particle can eventually chase light signal arbitrarily close. As for the central mass M of fig. (1), if this is a black hole then this criterium is fulfilled. But there is a more concrete set of particles in the Universe that match the ESP CP criteria relative to fig. (1), the high energy cosmic rays. The earth is continuously bombarded by these particles, some of them extragalactic others originating from the black hole region of our own galaxy, all with ultra high energies (Thoudam, S. et al., 2016; HESS Collaboration, 2016; The Pierre Auger Collaboration, 2017). On a cosmic scale, the subset of these particles that are observed on earth can be treated as moving towards the earth parallel to galactic and extragalactic photons, thus on a radial CP geodesic.

As for the EPS move away from clocks towards test-particles, we propose to connect this

to the move away from synchronization towards syntonization (*"syntonized" means "having equal frequencies" (Ashby et al., 2007)*). Einstein focused on synchronization procedures, todays technology more on syntonization.

> *It should be clear now that the difficulties inherent in the chronometric approach [...] are absent from the test-particle approach presented here, and that the latter approach offers a deeper understanding of the space-time geometry than the former. (Ehlers et al., 2012)*

From a phenomenological perspective this can be interpreted as the realization by EPS that real stable atoms do not carry time, only oscillatory frequencies. Chronometric devices as atomic clocks are human constructions based upon those atomic oscillations. Synchronized clocks are not fundamental objects in nature, syntonized oscillators are. The basic observable in an EPS approach should be atomic frequencies related to atoms, not synchronized time related to clocks.

According to (Capozziello et al., 2012), the Ehlers-Pirani-Schild formalism *provides a natural interpretation of the observables showing how relate them to General Relativity and to a large class of Extended Theories of Gravity.* In this paper, I connect the EPS approach intuitively and pragmatically to my Free Fall Grid approach towards gravitational phenomena. In fig. (1), the basic geodesics relative to a GNSS system are depicted, together with two positions A and B. The P geodesics are the satellite's free fall orbits around the earth's central mass M. The CP geodesics are the C or null geodesics of light- or EM-signal communication between posts A and B, but are at the same time the P or time like geodesics of freely falling Einstein elevators, thus the CP geodesics in the Free Fall Grid approach. In the following four sections I will gradually setup an EPS-FFG background structure that will be used to connect foreground GNSS precision atomic oscillator clocks.

IV.   A RECTANGULAR LATTICE OF SYNTONIZED STATIC CLOCKS IN FREE SPACE

This buildup starts with an Euclidian grid to which a Minkowski metric connection will be added. In the context of this paper, a grid is defined as frequency gauged localities, Einstein Elevators, spread out on a global structure in space and time, thus covering a four

dimensional event area. The Einstein Elevators contain frequency gauged clocks that can emit and absorb frequency gauged photons. A collection of such frequency gauged clocks is a syntonized ensemble, a grid. Additional synchronization is not assumed, all that needs to be monitored in the standard clocks is the frequency of the photons emitted or absorbed by the atomic oscillator being at rest in its core.

I assume that these clocks can also measure frequency shifts of received photons, using a Pound and Rebka type measurement of frequency difference to the highest accuracy (Pound and Rebka, G. A. Jr., 1960). And the Einstein Elevators are Einstein Equivalence Principle (EEP) local environments (Will, 2010). I will come back to the EEP in detail later in this paper. In the first example of a grid, the Einstein Elevators will be distributed on a rectangular, static lattice in free space, the Euclidian grid to which a Minkowski metric relating the Einstein Elevators will be added.
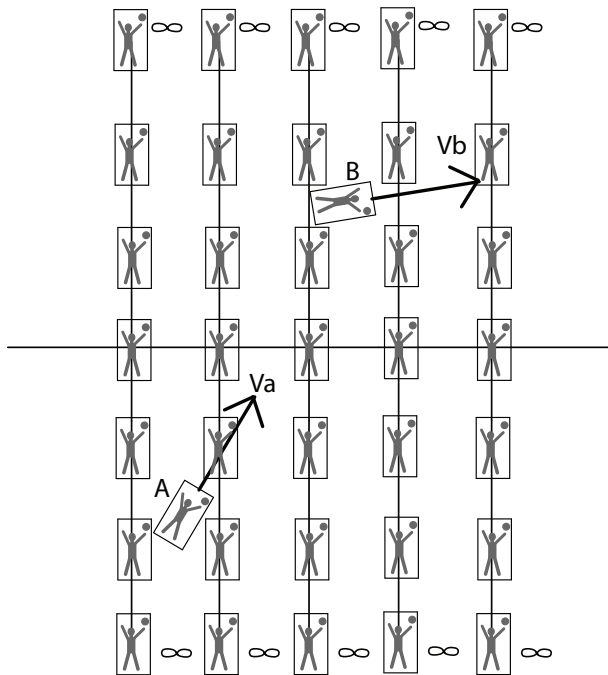

FIG. 2. Einstein Elevators in free space on a rectangular Euclidean lattice. The two randomly directed Einstein elevators A and B on the foreground each have a constant velocity v_a and v_b relative to this Euclidian grid that is their background.

Then a set of separate clocks A and B is introduced. These two clocks are not on this grid but move inside Einstein Elevators through this grid with two different random constant velocities, see fig.(2). From the fact that clocks on the grid aren't capable of directly

absorbing the photons emitted by the moving clocks, it can be inferred that these clocks on Einstein Elevator boxes A and B are operating on different frequencies, although they have the same standard clocks. Randomly moving standard clocks aren't frequency gauged with the grid.

Suppose we do not know how the clocks A and B are ticking relative to each other but we do have a procedure of how to relate the frequencies of the individual clocks A and B to the grid. Then we are also able to compare the clocks A and B relative to each other, as seen from the perspective of the grid.

So let the frequency of all the clocks on our grid be ν_g and let there be the two clocks A and B who are not on the grid and who have frequencies ν_a and ν_b. Suppose we know how to relate the frequency of clocks on the grid to the frequencies of clocks A and B as in

$$\frac{\nu_a}{\nu_g} = \delta_a \qquad and \qquad \frac{\nu_b}{\nu_g} = \delta_b, \tag{1}$$

so with measured values δ_a and δ_b. Then we also know how to relate the frequency of clock A directly to the one of clock B, as deduced from the grid perspective. We have, in an Euclidian environment,

$$Euclidian\ connection: \qquad \boxed{\frac{\nu_b}{\nu_a} = \frac{\delta_b}{\delta_a}.} \tag{2}$$

Next, imagine that we know how to Lorentz boost clocks from the grid to a position at rest right next to the off-the-grid clocks A and B with frequencies ν_a and ν_b. For such a Lorentz boost, we need to know the velocities v_a and v_b of the elevators A and B relative to the grid and then the Lorentz boost factors γ_a and γ_b can be calculated using

$$\gamma_a = \frac{1}{\sqrt{1 - \frac{v_a^2}{c^2}}}. \tag{3}$$

From Special Relativity we then have for clock-frequencies (Einstein, 1907),

$$\nu_a = \frac{1}{\gamma_a}\nu_g, \tag{4}$$

leading to

$$\frac{\nu_a}{\nu_g} = \frac{1}{\gamma_a} = \delta_a. \tag{5}$$

For the clock B we have equal equations relative to our grid. We insert these two known Lorentz boost into Eqn.(2) to get

$$Minkowski\ connection: \qquad \boxed{\frac{\nu_b}{\nu_a} = \frac{\gamma_a}{\gamma_b},} \tag{6}$$

with Lorentz boosts γ_a and γ_b both relative to the grid. We need the Minkowski metric to connect clocks on A and B to the grid and then to each other. An alternative way to present this result is

$$\frac{\Delta\nu_{ba}}{\nu_a} = \frac{\gamma_a - \gamma_b}{\gamma_b} \tag{7}$$

All we need to use Eqn.(6) or Eqn.(7) is a background of frequency gauged ensemble of standard clocks with on its foreground two non-gauged standard clocks with known Lorentz boosts relative to this background grid. This approach of relating two non-gauged foreground observers through a gauged grid in the background will be repeated throughout this paper.

V.   A RADIAL LATTICE OF STATIC CLOCKS AROUND A CENTRAL MASS

The procedure of the previous section also works using a radial instead of a rectangular grid in free space, see fig.(3). This is the basic grid used by a GNSS, and A and B can be satellites, airplanes, cars or shoppers with a smart-phone searching a specific store. There is however a problem with such a grid once it has a central mass in its center.

> *Present navigation satellite systems, such as Galileo and GPS, employ Newtonian trigonometry to determine positions, using Earth stations as reference points. This approach would perform ideally if all the satellites and the receiver were at rest and far from Earth.*
>
> *However, this is only correct as a first approximation because of the level of precision needed by a GNSS, the distortions that Earth causes in nearby space and time (space-time curvature) and the effects of the relative motions between the satellites and the user (relativistic inertial effects) both have to be considered. (ESA, 2010)*

Once a central mass M is added to the central Euclidian grid of fig.(3), clocks at a different radius from the center of M cannot absorb each others photons any more, see fig.(4). Then the system cases to be a globally frequency gauged lattice, it cases to be a global grid. This means that Special Relativity alone has limited use on this grid around a central mass, because in Special Relativity only velocity can influence the frequency of standard clocks and the clocks around M are all stationary. Clocks static relative to each other and on
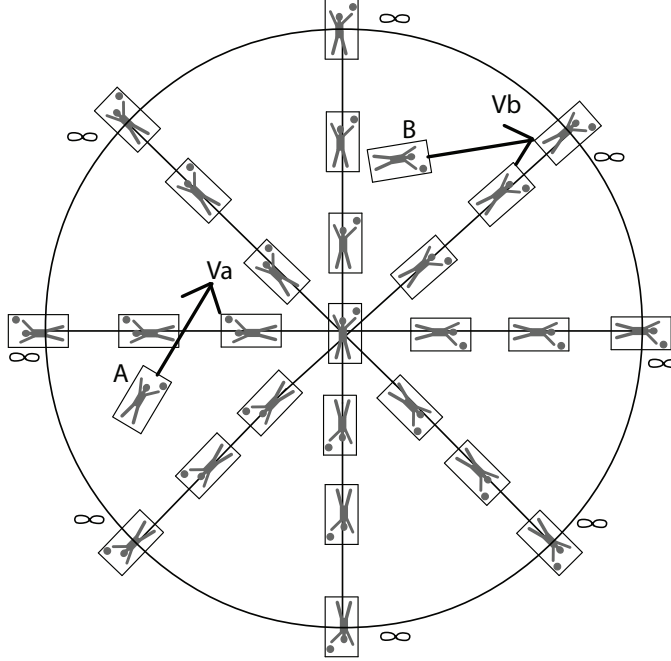
FIG. 3. Einstein Elevators in free space on a central static Euclidean syntonized lattice provide the background against which two randomly directed Einstein elevators A and B on the foreground are compared and connected. Such a grid is used in GNSS, where syntonization is assumed to be achieved during the factory setting of the atomic clocks as part of the production process. SR and GR effects are treated as corrections to this basic syntonization.

the same P-geodesic will still be syntonized, and so will clocks on the earths geoid (Ashby, 2002), but static clocks on Einstein Elevators on different P geodesics aren't syntonized.

Because static clocks on different P geodesics will be non-gauged, the global grid is lost. *It is well known that in general relativity global synchronization of clocks in gravitational field with no symmetries is impossible in principle. (Kheyfets, 1991)* This is the basic problem for relativistic GNSS. The Newton-Euclidian approach still assumes a global grid as its background. In GR-Schwarzschild, this actual global grid of real clocks as an imperfect reference system is replaced by an abstract metric, without having made clear to the technicians how to handle this loss.

In a stationary lattice around a central mass M, one locally has Einstein Elevators in which Special Relativity can be applied, because EEP is valid in them. But we cannot use Special Relativity alone to connect the standard clocks in the Einstein Elevators to each other on the global scale. Gravity disintegrates the Euclidian static grid, even with
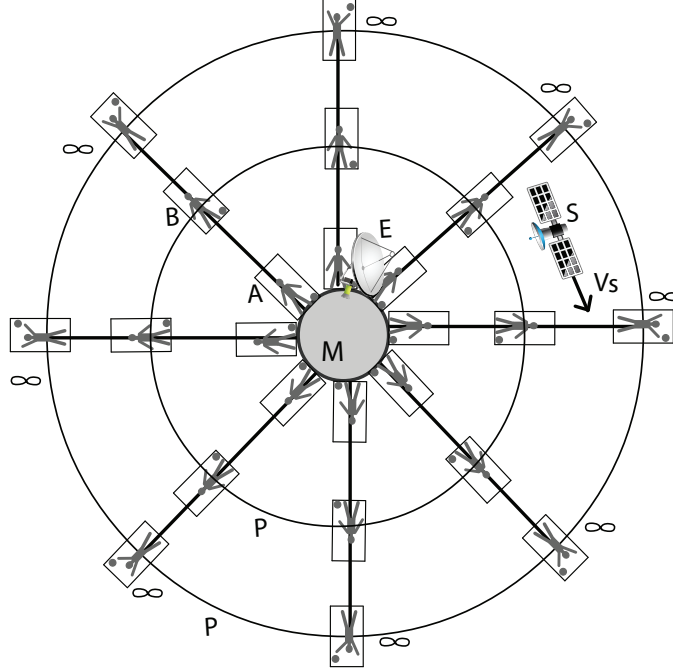
FIG. 4. A background of Einstein Elevators in a stationary lattice around a central mass M, including a GPS satellite S and an GPS earthbound station E on the foreground. Only the background Einstein Elevators on the same P geodesic can function as a limited syntonized P grid. The problem is how to connect atomic clocks on different P-geodesics, in the absence of a truly global grid.

a Minkowski metric, into separately syntonized P geodesics. Different GNSS systems are orbiting the earth on different heights, thus also on different P geodesics. This implies that we cannot relate the frequencies of the standard clocks on the Einstein Elevator Satellite S and Einstein Elevator Earth ground Station E on the foreground to this radial lattice as the background. On a global scale the background isn't syntonized any more.

Kheyfets suggested to use what he called 'Schwarzschild coordinate time' to realize a global synchronization scheme.

> It would be a good idea to make all the clocks to display Schwarzschild coordinate time, i. e. the time of an observer placed at spatial infinity and resting with respect to the Schwarzschild coordinates. Schwarzschild coordinate time is the closest possible analog of the time of the ECI frame (the special relativistic limit of the Schwarzschild coordinate frame coincides with the ECI frame). The first step in this direction is to compare the rates of the clocks of the satellite and the

14

observer with Schwarzschild clocks simultaneously with respect to Schwarzschild time. (Kheyfets, 1991)

The proposal of Kheyfets would imply to synchronize all the clocks of the stationary observers in Fig. (4) to the clocks of the stationary observers at infinity. Kheyfets wants to use the Schwarzschild metric as the global background, thus imposing this metric upon all static observers as a synchronization scheme. To first order in Φ/c^2 this equals the Newton-Euclician approach, with the difference that in the last globalization method, the Earth based factory setting is used as the globally enforced time and not the stationary time at infinity.

The Free Fall Grid approach of this paper has a strong connection to Kheyfets' because I use 'Schwarzschild coordinate time'-rate to realize a global syntonization scheme. This syntonization scheme isn't enforced upon the stationary lattice of Fig. (4). I introduce a Free Fall Grid on radial CP geodesics as a replacement of the Newton-Euclidian pre-relativistic radial grid and as a global background for the tangential P-geodesics around a central mass. This EPS-FFG background, in the form of a Minkowski-EEP grid, might be a pragmatic intermediate towards a fully operational curved metric background for GNSS.

VI. FROM THE EINSTEIN EQUIVALENCE PRINCIPLE TO THE FREE FALL GRID

I combine the Minkowski metric with the Einstein Equivalence Principle (EEP) to construct an hypothetical alternative grid for global GNSS purposes, the Free Fall Grid. At this point a clarification of what is meant by the EEP is at place. There are three versions of the equivalence principle in physics. The equivalence of being at rest in free space and being in free fall in a field of gravity is what is called the weak equivalence principle (WEP). In a free falling elevator, the resulting local space-time must be Minkowskian. Einstein added what is now called the strong equivalence principle (SEP) to the Galilean notion of free fall. The SEP states the equivalence of an accelerated frame and uniform gravity. A uniform acceleration in free space can be replaced by a gravitational field that is homogeneous in the first order, thus giving the observer the impression of being at rest in a field of gravity instead of being in a state of accelerated motion in free space. Einstein derived the gravitational red shift from this second equivalence principle. Uniform gravity only exists as a local

idealization. The real gravitational field of a stationary central mass cannot be transformed away globally, all around that central mass (Einstein, 1916; Norton, 1985).

My approach is based upon the Weak Equivalence Principle or the principle of free fall. I don't use the Strong Equivalence Principle of homogeneous gravity and constant acceleration. It does imply the Local Lorentz Invariance (LLI), which states that locally special relativity is valid and is not affected by the presence of a gravitational field. In the free fall elevators atomic oscillators are assumed to be present, as clock frequency generators, to remain frequency gauched from infinity all the way towards the central mass M. Therefore Local Position Invariance or LPI must be valid on these Einstein Elevators. Local Position Invariance implies that the non-gravitational constants of nature are space-time independent. WEP, LLI and LPI are the three pillars of the Einstein Equivalence Principle (EEP) (Will, 2014; Wolf et al., 2017). The Einstein elevators of this paper are all assumed to embody the Einstein Equivalence Principle when in geodesic, force free motion.

In physics, there is a long history of deducing gravity effects using Special Relativity and EEP, as for example in (Ashby, 2006). In this paper I continue that tradition, which was also at the core of my previous paper, in which I derived the geodesic precession using hyperbolic Special Relativity and EEP (de Haas, 2014). In the SR-EEP Einstein Elevators in free-fall the following applies:

> Inside a freely falling elevator, as long as the field is uniform (locally), they would be subject to zero total force, which is equivalent to being inside an elevator at rest in empty space (or moving with uniform velocity), in which case there would be no frequency shift. (Nobili et al., 2013)

In other words, an atomic clock placed in an Einstein Elevator at rest in infinity and then set on a free fall trajectory towards a central mass M, will, all the way down to M remain at the same initial rest system frequency. Tests of the WEP (part of EEP) in free fall have reached accuracies comparable to the accuracy of atomic clocks (Will, 2014). Atomic clocks on "Einstein Elevators" in free fall from at rest in infinity towards a central mass on a radial CP geodesic will remain frequency gauged or syntonized all the way down towards M. In this way a free fall ensemble of syntonized clocks capable of emitting syntonized photons is established.

All free falls start at rest in infinity and stretch all the way to just above the surface of
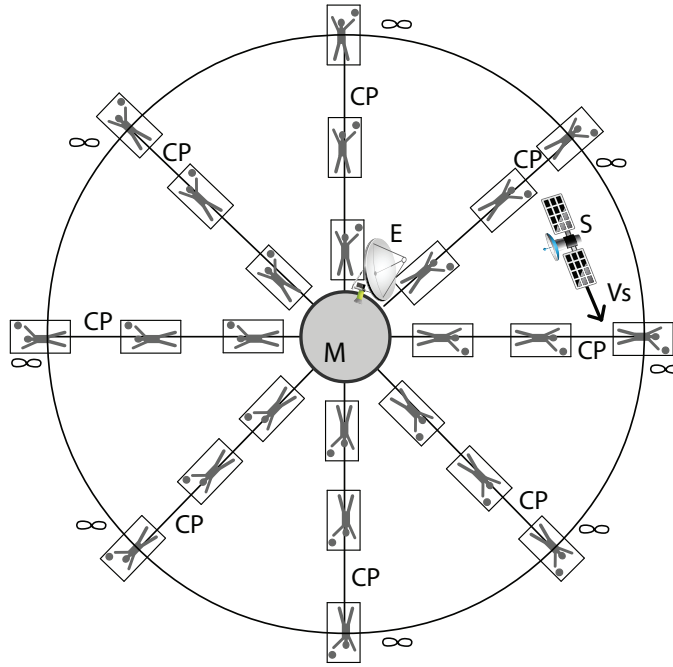
FIG. 5. A CP background of Einstein Elevators in free fall on a global free fall grid, a CP-FFG, on which Special Relativity is valid. On the foreground a GNSS satellite in a geodesic P orbit around M and a stationary GNSS ground station on another P geodesic (the Earth's geoid) are also depicted. In our EPS approach, the foreground E and S will be related through the background FFG grid, using two CP-P connections.

this central mass, see fig.(5). On this grid one has an infinite number of Einstein Elevators in perfect free fall. All the clocks at rest in the Einstein Elevators on this free fall grid (FFG) have rest system frequency $\nu_g = \nu_0 = \nu_\infty$. These clocks do not feel any acceleration. Without acceleration there is no Lorentz boost, and without Lorentz boost the clock frequency will not change. Thus the FFG of figure (6) constitutes a perfect example of a global ensemble of frequency gauged clocks, a global grid.

So all the clocks on the grid can absorb photons emitted by all the other clocks on the grid, although the velocity of the clocks varies with height in the perspective of observers who are stationary relative to the central mass M. From the perspective of this grid, gravity does not exist and the velocity of light is a constant in all directions. In the terminology of EPS, this radial FFG constitutes a CP structure and this grid spans a Weyl Space.

This free fall grid is not very practical in performing scientific experiments. Rohrlich

started a 1963 paper on the principle of equivalence with the observation that it was very difficult to perform laboratory experiments in falling elevators. They were usually carried out in reference frames that were supported in a static gravitational field (Rohrlich, 1963). Half a century later, such a free fall research lab do exist, as for example the Bremen Drop Tower of the ZARM laboratories, with a height of 146 meter (Seibert and Fitton, 2001). The difference with the FFG is that ZARM's Drop Tower free fall doesn't start at infinity. Because of that, the CP-FFG can only function as a theoretical instrument, an instrument of calculus, useful to relate real clocks, as for example clocks A and B in fig. (6).

VII.   THE FREE FALL GRID CONNECTING TWO STATIC CLOCKS.

These clocks A and B in Einstein Elevators are on a stationary lattice at a definite radial distance from the center of mass M, see fig.(4) and fig. (6). Observer A is closer to the central mass M than observer B. The observers A and B feel the pull of gravity induced acceleration on their clocks. As they try to exchange photons, they find out that the received photons are not being absorbed, meaning that the photons of the other atomic oscillator based clock are frequency shifted relative to their own clock, although they were send by a clock with identical factory settings.

The only difference is the height, the vertical position of the emitting clock. They conclude that gravity is negatively influencing the procedure of establishing a frequency gauged lattice. When they bring their clocks next to each other, either by A going to B or B going to A, the clocks are again absorbing each others photons, thus ensuring the frequency gauged original situation and confirming LPI. But as soon as they move up or down again with their clocks, photons case to be absorbed and they cannot achieve a frequency gauged global grid. This is the situation of the experiment performed by Pound and Rebka in 1960 (Pound and Rebka, G. A. Jr., 1960), more specific, the part prior to the application of a correcting Doppler shift.

In order to bring some clarity to this situation we imagine a free fall grid (FFG) as the background of the stationary lattice with observers A and B, see fig.(6). Using the conservation of energy and Special Relativity we can relate the clocks A and B on the stationary lattice to clocks on the FFG. Relativistic kinetic energy is defined as $U_k = (\gamma - 1)U_0$ (Rindler, 2001, p. 112), in which $U_0 = m_0 c^2$ is the rest energy. Gravitational potential energy is given
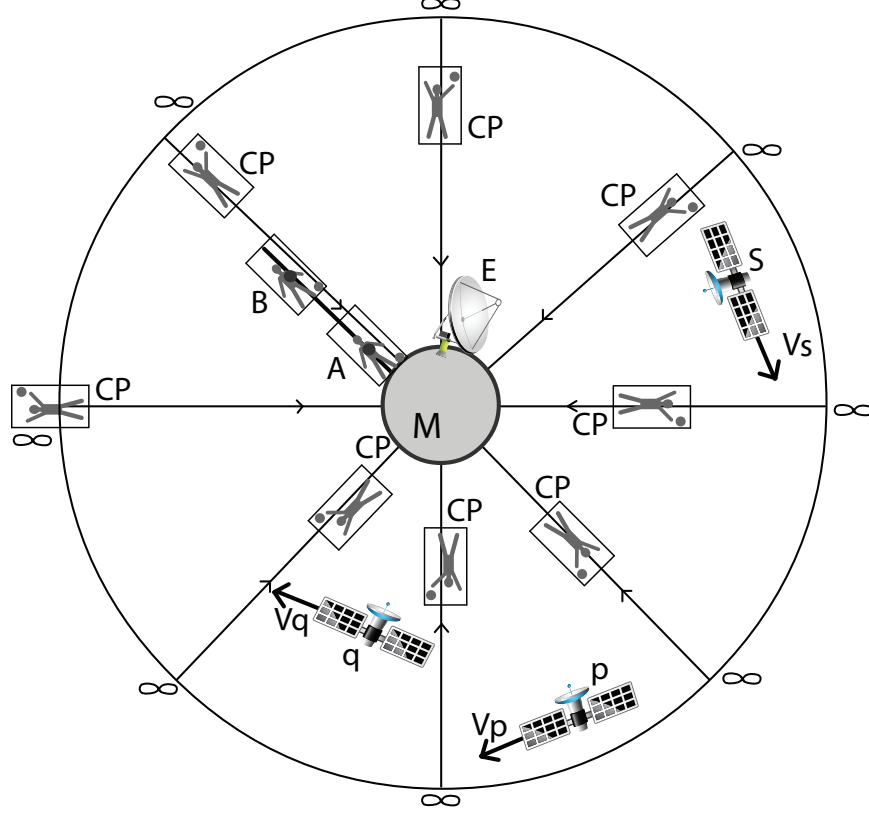
FIG. 6. Background Einstein Elevators in free fall on the CP-FFG with a foreground set of two stationary Einstein Elevators A and B located on different P geodesics. Another foreground set is given by the GNSS ground station E and an orbiting satellite S. The two satellites p and q will figure in the Inter Satellite Link section. Einstein Elevators A, B and E are not in free fall on P, the satellites S, p and q are.

by $U_\phi = m_0\Phi$, with Φ as the Newtonian potential. Relative to the stationary clocks the Einstein Elevator in free fall has relativistic kinetic U_k. Due to energy conservation, potential energy and kinetic energy relate as $U_k = -U_\phi$ because the free fall started at infinity. This results in the Lorentz boost connection between a locally passing by elevator on the FFG and a clock on the stationary lattice as $(\gamma_\phi - 1)m_0 c^2 = -m_0\Phi$, so one gets

$$\gamma_\phi = 1 - \frac{\Phi}{c^2}. \tag{8}$$

A passing by elevator on the FFG can always position or launch a clock from his elevator next to a clock on the stationary lattice by such a Lorentz boost, at least momentarily. In

19

the classical velocity and energy range, we have $U_k = -U_\phi$ leading to

$$\frac{1}{2}v_\phi^2 = -\Phi \qquad \Leftrightarrow \qquad v_\phi^2 = -2\Phi \tag{9}$$

On might be tempted to relate the two clocks on the stationary grid to each other through the intermediate of clocks on the free fall grid using Eqn. (6), $\nu_b/\nu_a = \gamma_a/\gamma_b$. Eqn. (6) howerer can't reproduce the basic gravitational experimental facts. Eqn. (6) was obtained with an Euclidian grid at rest with two moving clocks within Einstein Elevators, related to the grid through the Minkoswki metric. But now we have moving clocks on the frequency gauged grid, the CP-FFG, and clocks at rest on P-geodesics of the stationary lattice. This reversal of roles needs careful attention. If we write ν_{ga} for frequency of the clock on the CP-grid falling by the clock at rest in A on the P-grid with frequency ν_{0a}, relative velocity v_a and relative boost γ_a we get

$$\nu_{ga} = \frac{1}{\gamma_a}\nu_{0a}, \tag{10}$$

resulting in $\nu_{0a} = \gamma_a\nu_{ga}$. For clock B we can do the same, after which we can calculate ν_{0b}/ν_{0a} as

$$\frac{\nu_{0b}}{\nu_{0a}} = \frac{\gamma_b\nu_{gb}}{\gamma_a\nu_{ga}} = \frac{\gamma_b}{\gamma_a}. \tag{11}$$

The last step is possible because the clocks on the Free Fall Grid ν_{0b} and ν_{0a} are still frequency gauged and the clocks on the stationary grid are not. This is the reversal of the situation in the gravity free world, were clocks at rest can be frequency gauged and the clocks in different states of motion cannot be frequency gauged. The reversal doesn't affect applied laws of physics but it does make the difference between Minkowski and Minkowski-EEP.

Writing ν_{0a} as ν_a again, we get

$$\boxed{Minkowski-EEP: \qquad \frac{\nu_b}{\nu_a} = \frac{\gamma_b}{\gamma_a}}, \tag{12}$$

in which the γ's have to be interpreted as Einstein Elevator local CP-P connections.

For clocks with non relativistic virtual escape velocity in a Newtonian field of gravity, so $v^2 = -2\Phi$, this leads to

$$\frac{\nu_b}{\nu_a} = \frac{\gamma_b}{\gamma_a} = \frac{\sqrt{1-\frac{v_a}{c^2}}}{\sqrt{1+\frac{v_b}{c^2}}} = \frac{\sqrt{1+\frac{2\Phi_a}{c^2}}}{\sqrt{1+\frac{2\Phi_b}{c^2}}} = \frac{\sqrt{1-\frac{2GM}{r_a c^2}}}{\sqrt{1-\frac{2GM}{r_b c^2}}}. \tag{13}$$

This is the exact GR Schwarzschild stationary redshift (Rindler, 2001, p. 236; Carrol, 2004, p. 217; Ohanian and Ruffini, 2013, p. 308). To first order in $\frac{\Phi}{c^2}$ this leads to the familiar

$$\frac{\nu_b}{\nu_a} \approx \left(1 - \frac{\Phi_b}{c^2}\right)\left(1 + \frac{\Phi_a}{c^2}\right) = 1 + \frac{\Delta\Phi_{ab}}{c^2} + \mathcal{O}(c^{-4}). \tag{14}$$

and to

$$\frac{\Delta\nu_{ba}}{\nu_a} = \frac{\Delta\Phi_{ab}}{c^2}. \tag{15}$$

When clocks A and B are close to each other relative to the distance R to the centre of M, $\Delta r \ll r$, one has

$$\frac{\Delta\nu_{ba}}{\nu_a} = \frac{gh}{c^2} \tag{16}$$

with h as the distance between the clocks A and B. As a result, the frequency of the clock at A will be lower than the frequency of the clock B who is positioned less deep in the gravitational field than clock A. This General Relativity prediction matched the experimental result obtained by Pound and Rebka in 1959, in the form of a correcting Doppler shift of this magnitude, and by others thereafter (Will, 2014).

VIII.   THE FREE FALL GRID SECOND ORDER IN Φ/c^2 STATIC REDSHIFT

Now that I reproduced the exact GR-Schwarzschild results for weak field redshifts, I can make a second order in ϕ/c^2 red shift prediction based on the FFG approach. The FFG second order in ϕ/c^2 gravitational redshift between two stationary clocks at different heights reads

$$\frac{\nu_b}{\nu_a} = \frac{\gamma_b}{\gamma_a} = \frac{1 - \frac{\Phi_b}{c^2}}{1 - \frac{\Phi_a}{c^2}} \approx \left(1 + \frac{\Phi_a}{c^2} + \frac{\Phi_a^2}{c^4} + \mathcal{O}(c^{-6})\right)\left(1 - \frac{\Phi_b}{c^2}\right) = \tag{17}$$

$$1 + \frac{\Delta\Phi_{ab}}{c^2} + \frac{\Phi_a}{c^2}\frac{\Delta\Phi_{ab}}{c^2} + \mathcal{O}(c^{-6}) = 1 + (1 + \frac{\Phi_a}{c^2})\frac{\Delta\Phi_{ab}}{c^2} + \mathcal{O}(c^{-6}). \tag{18}$$

If the the third order in ϕ/c^2 and higher terms are omitted, given by $\mathcal{O}(c^{-6})$, one gets, after a bit of reshuffling,

$$\boxed{Minkowski - EEP: \quad \frac{\Delta\nu_{ba}}{\nu_a} = (1 + \frac{\Phi_a}{c^2})\frac{\Delta\Phi_{ab}}{c^2}} \tag{19}$$

In General Relativity this is given by

$$\frac{\nu_b}{\nu_a} = \frac{\sqrt{g_{00}^a}}{\sqrt{g_{00}^b}} = \frac{\sqrt{1 + \frac{2\Phi_a}{c^2}}}{\sqrt{1 + \frac{2\Phi_b}{c^2}}} \approx \left(1 - \frac{\Phi_b}{c^2} + \frac{3\Phi_b^2}{2c^4}\right)\left(1 + \frac{\Phi_a}{c^2} - \frac{\Phi_a^2}{2c^4}\right) = \tag{20}$$

$$1 + \frac{\Delta\Phi_{ab}}{c^2} - \frac{\Phi_b}{c^2}\frac{\Delta\Phi_{ab}}{c^2} + \frac{\Phi_b^2}{2c^4} - \frac{\Phi_a^2}{2c^4} + \mathcal{O}(c^{-6}). \tag{21}$$

If again we omit the third order in ϕ/c^2 and higher terms, given by $\mathcal{O}(c^{-6})$, and rewrite it we get the second order GR-Schwarzschild static redshift as

$$\boxed{GR - S: \quad \frac{\Delta\nu_{ba}}{\nu_a} = (1 - \frac{\Phi_b}{c^2})\frac{\Delta\Phi_{ab}}{c^2} + \frac{\Phi_b^2}{2c^4} - \frac{\Phi_a^2}{2c^4}.} \tag{22}$$

To first order in ϕ/c^2 the EPS-FFG approach, Eqn. (19), gives the same result as the GR-Schwarzschild approach, Eqn. (22). This can be written as

$$\frac{\Delta\nu_{ba}}{\nu_a} = (1 + \alpha)\frac{\Delta\Phi_{ab}}{c^2}, \tag{23}$$

with $\alpha = 0$ to the first order accuracy if LPI is valid (Turneaure et al., 1983; Delva and Lodewyck, 2013; Will, 2014; Wolf et al., 2017). Once experimental redshift tests of LPI reach second order in ϕ/c^2 accuracy, the deviation term has to be upgraded to second order too, which, for the EPS-FFG approach, by writing this term as α' results in

$$\frac{\Delta\nu_{ba}}{\nu_a} = \frac{\Delta\Phi_{ab}}{c^2} + (1 + \alpha')\frac{\Phi_a}{c^2}\frac{\Delta\Phi_{ab}}{c^2}, \tag{24}$$

with $\alpha' = 0$ to the second order accuracy if LPI is valid. If nothing is changed in the redshift LPI test formulation, then EPS-FFG and GR-Schwarzschild both predicts $|\alpha| \approx 10^{-10}$. But then this value of $\alpha \neq 0$ has to be interpreted as a confirmation of LPI. To avoid confusion, it would be better to shift to the α' formulation of second order redshift LPI tests somewhere the next decades.

The difference between the second order static redshift predictions of EPS-FFG and GR-Schwarzschild might be related to the question of how weak a field of gravity actually is when you go to second order in ϕ/c^2 accuracy. In the EPS-FFG approach, virtual escape velocities determine the static redshift and a shift from Newtonian kinetic energy to SR kinetic energy seems appropriate in the second order in ϕ/c^2 accuracy range. In the GR-Schwarzschild approach, the static redshift has obviously nothing to do with velocity, only with strength of gravity/curvature. In the Newtonian kinetic/gravitational escape energy range, the two approaches are identical.

In the PPN approach, a perturbation of the weak-field Schwarzschild metric is used for the higher order field strengths (Castel-Branco et al., 2014), giving for g_{00} the second order extension

$$g_{00} = 1 + \frac{2\Phi}{c^2} + 2\beta \left(\frac{\Phi}{c^2}\right)^2 \tag{25}$$

leading to a second order gravitational redshift

$$\frac{\nu_b}{\nu_a} = \frac{\sqrt{g_{00}^a}}{\sqrt{g_{00}^b}} = \frac{\sqrt{1 + \frac{2\Phi_a}{c^2} + 2\beta \left(\frac{\Phi_a}{c^2}\right)^2}}{\sqrt{1 + \frac{2\Phi_b}{c^2} + 2\beta \left(\frac{\Phi_b}{c^2}\right)^2}} \tag{26}$$

and to the PPN result

$$PPN: \quad \frac{\Delta\nu_{ba}}{\nu_a} = (1 - \frac{\Phi_b}{c^2})\frac{\Delta\Phi_{ab}}{c^2} + (1 - 2\beta)\left(\frac{\Phi_b^2}{2c^4} - \frac{\Phi_a^2}{2c^4}\right) \tag{27}$$

with $\beta = 0$ for GR-Schwarzschild.

Present day accuracy of the gravitational redshift measurements goes to $\alpha < 10^{-6}$ (Ashby et al., 2007; Will, 2014; Wolf et al., 2017). In the following decades the accuracy of the stationary redshift measurements should be such that α measurements are going to reach the 10^{-10} relative accuracy. Given the speed of development, it might even be sooner than later. The second order terms in the gravitational redshift calculations presented above are in the 10^{-10} range of α and in the 10^{-20} accuracy range of the redshift itself. Of these calculations, the first two are theoretical predictions. In the PPN calculation, the 'free' parameter β can be adjusted to approach the measurements as close as possible. As such, the PPN approach is the most flexible and the less predictive of the three.

IX. THE FFG CONNECTING A SATELLITE AND A GROUND STATION

In figure (6) I also depicted a GPS ground station E and a GPS satellite S. In this section I will use our method to derive the relative frequency shift between the standard clock on the satellite S compared to the standard clock on the ground station E. In order to do this using eqn.(12), I need the two gamma factors, of both the ground station E and the orbiting satellite S, relative to our free fall grid. I already used the first gamma factor in the previous derivation: $\gamma_e = 1 - \frac{\Phi_e}{c^2}$. For the second gamma factor I will use a result already arrived at in a previous paper. In (de Haas, 2014) I used hyperbolic relativity to derive the Lorentz boost connection between an observer locally passing by on a free fall grid and an orbiting

23

satellite. It was shown that two successive boosts could launch a satellite from the FFG elevator into a stable orbit around M. The first boost gave the satellite an escape amount of kinetic energy U_{esc} relative to the free fall elevator and the second boost, perpendicular to the first, gave it an orbital kinetic energy U_{orb}. Using relativistic kinetic energy U_k one gets

$$\gamma_{esc} = 1 - \frac{\Phi}{c^2}. \tag{28}$$

From the conservation of energy and the virial theorem results

$$\gamma_{orb} = 1 - \frac{\Phi}{2c^2}. \tag{29}$$

Under the condition that the two boosts are perpendicular relative to each other this results in the Lorentz boost connection between the FFG and the satellite as

$$\gamma_{sat} = \gamma_{esc}\gamma_{orb} = \left(1 - \frac{\Phi}{c^2}\right)\left(1 - \frac{\Phi}{2c^2}\right) = 1 - \frac{3\Phi}{2c^2} + \frac{\Phi^2}{2c^4} \approx 1 - \frac{3\Phi}{2c^2}, \tag{30}$$

as has been applied, using standard hyperbolic Special Relativity, in (de Haas, 2014).

This hyperbolic addition of Lorentz boosts is based on the addition of rapidities. Given the definition of rapidity φ through $\beta = \tanh\varphi$ with $\beta = v/c$, $\gamma = \cosh\varphi$ and $\gamma\beta = \sinh\varphi$, the Lorentz boost addition law as formulated by (Varičak, 1912) reads

$$\cosh(\psi) = \cosh(\varphi_1)\cosh(\varphi_2) + \sinh(\varphi_1)\sinh(\varphi_2)\cos(\alpha), \tag{31}$$

with the angle α as the angle between the two velocity vectors themselves. Translated to Lorentz boosts as given by γ and β, this relativistic velocity addition rule can be written as

$$\gamma_\psi = \gamma_{\varphi_1}\gamma_{\varphi_2} + \gamma_{\varphi_1}\beta_{\varphi_1}\gamma_{\varphi_2}\beta_{\varphi_2}cos(\alpha). \tag{32}$$

When the two velocities are perpendicular, $cos(\alpha) = 0$ and this reduces to $\gamma_\psi = \gamma_{\varphi_1}\gamma_{\varphi_2}$.

Now that the hyperbolic part of Eqn. (30) has been justified we can combine Eqn. (12) and Eqn. (30) to get

$$\frac{\nu_s}{\nu_e} = \frac{\gamma_s}{\gamma_e} = \frac{1 - \frac{3\Phi_s}{2c^2} + \frac{\Phi_s^2}{2c^4}}{1 - \frac{\Phi_e}{c^2}} \approx \tag{33}$$

$$\left(1 + \frac{\Phi_e}{c^2} + \frac{\Phi_e^2}{c^4} + \mathcal{O}(c^{-6})\right)\left(1 - \frac{3\Phi_s}{2c^2} + \frac{\Phi_s^2}{2c^4}\right) = \tag{34}$$

$$1 + \frac{\Delta\Phi_{es}}{c^2} - \frac{\Phi_s}{2c^2} + \frac{\Phi_e}{c^2}\left(\frac{\Delta\Phi_{es}}{c^2} - \frac{\Phi_s}{2c^2}\right) + \frac{\Phi_s^2}{2c^4} + \mathcal{O}(c^{-6}) = \tag{35}$$

$$1 + \left(1 + \frac{\Phi_e}{c^2}\right)\left(\frac{\Delta\Phi_{es}}{c^2} - \frac{\Phi_s}{2c^2}\right) + \frac{\Phi_s^2}{2c^4} + \mathcal{O}(c^{-6}). \tag{36}$$

If we omit the third order in ϕ/c^2 and higher terms, given by $\mathcal{O}(c^{-6})$, and rewrite it we get

$$\boxed{\frac{\Delta\nu_{se}}{\nu_e} = \left(1 + \frac{\Phi_e}{c^2}\right)\left(\frac{\Delta\Phi_{es}}{c^2} - \frac{\Phi_s}{2c^2}\right) + \frac{\Phi_s^2}{2c^4}}. \tag{37}$$

For future developments of relativistic GNSS based experiments and applications in second order in ϕ/c^2 accuracy range, Eqn. (37) is the relevant falsifiable/verifiable prediction of this paper. It can be compared to Eqn. (26) of (Jaffe and Vessot, 1976), a PPN second order redshift prediction. They proposed to measure this second order gravitational redshift by tracking a satellite in a highly eccentric orbit around the sun while comparing its frequency with an identical clock on earth (Jaffe and Vessot, 1973).

We can approximate Eqn. (37) even further, to first order in Φ/c^2, to get

$$\frac{\Delta\nu_{se}}{\nu_e} = \frac{\Delta\Phi_{es}}{c^2} - \frac{\Phi_s}{2c^2} \tag{38}$$

Classically, in the Newtonian low velocity situation and the virial theorem, the last term gives the kinetic energy. In terms of the Lagrangian $L = U_K - U_\Phi$ and atomic oscillator rest-mass m_0, we get

$$\frac{\Delta\nu_{se}}{\nu_e} = \frac{m_0\Delta\Phi_{es}}{m_0 c^2} + \frac{\frac{1}{2}m_0 v_s^2}{m_0 c^2} = \frac{L_s - L_e}{U_0}, \tag{39}$$

assuming that all clocks are produced identically and use the same atomic oscillator as their core. The almost non-relativistic velocities and the weak fields explains the appearance of the classical mechanical Lagrangian in the first order in Φ/c^2 relativistic redshift approximation. We thus have for the satellite-earth frequency difference

$$\frac{\Delta\nu_{se}}{\nu_e} = \frac{\Delta L_{se}}{U_0}. \tag{40}$$

The result of Eqn. (38) is the basic relativistic correction used in GNSS clock frequencies, with the first as the gravity effect or gravitational potential correction and the second as the velocity effect or the correction due to Special Relativity (Ashby, 2002; Hećimović, 2013; Delva and Lodewyck, 2013).

These first order in Φ/c^2 effect of height and velocity produce $\frac{\Delta\nu_{es}}{\nu_e} \approx 10^{-10}$, creating an accumulative clock-drift of about 40 $\mu s/day$ (Ashby, 2003; Bahder, 2003). This makes it relevant for todays GNSS. The additional second order effect is in the order of $\frac{\Delta\nu_{se}}{\nu_e} \approx 10^{-20}$. Todays precision clocks reach a relative accuracy of 10^{-17}. The gravitational redshift in the ACES/PHARAO experiment, which compares clock on the ISS with ground station clocks,

is expected to measure the absolute redshift such that the constraint on α wil be improved by a factor 45 compared to the GP-A experiment, resulting in $|\alpha| \approx 3 \cdot 10^{-6}$. The accuracy of the spaceborne and ground clocks used in the ACES/PHARAO experiment in order to reach this expected accuracy is about 10^{-16} (Wolf et al., 2017). Thus, in order for direct measurement of the relative frequency shift due to second order in Φ/c^2 contribution to the ordinary redshift, clocks with an accuracy of 10^{-20} are needed. Given the fact that clocks are improved by a factor 10 every decade (Delva and Lodewyck, 2013), and that such experiments take a decade of preparation time, it might still take four decades before second order effect become directly measurable. But accumulative effects in clock drift will speed up the relevancy for GNSS practices. In the analysis of (Delva and Lodewyck, 2013), clock accuracies of 10^{-19} will make it necessary to include c^{-4} terms.

X.   THE FFG CONNECTION BETWEEN TWO ORBITING SATELLITES

In the GNSS research community, the inter-satellite link (ISL) is a promising topic, a technique for enhancing GNSS reliability and integrity (Xie, 2016). In our EPS-FFG approach we can calculate the second order accuracy ISL. Given the exact FFG to satellite or CP-P connection as used in the previous section,

$$\gamma_{sat} = \gamma_{esc}\gamma_{orb} = 1 - \frac{3\Phi}{2c^2} + \frac{\Phi^2}{2c^4}, \tag{41}$$

we can also connect two satellites p and q to second order accuracy.

$$\frac{\nu_p}{\nu_q} = \frac{\gamma_p}{\gamma_q} = \frac{1 - \frac{3\Phi_p}{2c^2} + \frac{\Phi_p^2}{2c^4}}{1 - \frac{3\Phi_q}{2c^2} + \frac{\Phi_q^2}{2c^4}} \approx \tag{42}$$

$$\left(1 + \frac{3\Phi_q}{2c^2} + \frac{7\Phi_q^2}{4c^4}\right)\left(1 - \frac{3\Phi_p}{2c^2} + \frac{\Phi_p^2}{2c^4}\right) = \tag{43}$$

$$1 + \frac{3\Delta\Phi_{qp}}{2c^2} + \frac{3\Phi_q}{2c^2}\left(\frac{3\Delta\Phi_{qp}}{2c^2}\right) + \frac{\Phi_p^2}{2c^4} - \frac{\Phi_q^2}{2c^4} = \tag{44}$$

$$1 + \left(1 + \frac{3\Phi_q}{2c^2}\right)\left(\frac{3\Delta\Phi_{qp}}{2c^2}\right) + \frac{\Phi_q^2}{2c^4} - \frac{\Phi_p^2}{2c^4} \tag{45}$$

We can rewrite this as:

$$\boxed{FFG - ISL: \quad \frac{\Delta\nu_{pq}}{\nu_p} = \left(1 + \frac{3\Phi_q}{2c^2}\right)\left(\frac{3\Delta\Phi_{qp}}{2c^2}\right) + \frac{\Phi_p^2}{2c^4} - \frac{\Phi_q^2}{2c^4}} \tag{46}$$

For future developments of relativistic GNSS, this is our CP-P second order satellite to satellite, ISL, relativistic redshift prediction. As for its possible relevance, it is technically unavoidable that in the not to near future, both the GPS local P-grid and the Galileo local P-grid will become independent self-gauged P-grids. Eqn. (46) then gives a verifiable/falsifiable prediction regarding their frequency shift connection.

Now, let q be the satellite on the lower P geodesic and p the satellite in the higher one. The energy formulation of the CP-P redshift, which integrates the relativistic velocity and the relativistic gravity for the second order in Φ/c^2 and v^2/c^2 satellite-satellite redshift, includes all the simpler situations. We will use $V = U_\Phi$ and $K = U_k$ for potential and kinetic energy respectively. Given the factory assemblage of all clocks, we assume $m_p = m_q = 1$ and set $c = 1$. Using this, Eqn. (46) becomes

$$p_{sat} - q_{sat} : \quad \frac{\Delta\nu_{pq}}{\nu_p} = (1 + V_q - K_q)(\Delta V_{qp} - \Delta K_{qp}) + 2(K_q^2 - K_p^2). \tag{47}$$

The situation with satellite and earth ground station is given by taking away the kinetic energy of q:

$$p_{sat} - q_{earth} : \quad \frac{\Delta\nu_{pq}}{\nu_p} = (1 + V_q)(\Delta V_{qp} + K_p) - 2K_p^2. \tag{48}$$

The situation with an earth ground station at a higher location and another at a lower location is then given by taking away the kinetic energy of the other satellite:

$$p_{earth} - q_{earth} : \quad \frac{\Delta\nu_{pq}}{\nu_p} = (1 + V_q)(\Delta V_{qp}). \tag{49}$$

We can also go to first order in V accuracy for all three situations by removing the term in the first bracket and the end terms:

$$p_{sat} - a_{sat} : \quad \frac{\Delta\nu_{pq}}{\nu_p} = \Delta V_{qp} - \Delta K_{qp}; \tag{50}$$

$$p_{sat} - q_{earth} : \quad \frac{\Delta\nu_{pq}}{\nu_p} = \Delta V_{qp} + K_p; \tag{51}$$

$$p_{earth} - q_{earth} : \quad \frac{\Delta\nu_{pq}}{\nu_p} = \Delta V_{qp}. \tag{52}$$

This concise formulation in terms of energies sums up the redshift result of the CP-P EPS-FFG approach of this paper, including both kinematic and gravitational relativistic (time dilated) redshifts terms in an integrated way. In first order in V accuracy, the symmetry has a strong Lagrangian $L = K - V$ signature, especially in the satellite to satellite, or inter satellite link (ISL), relativistic redshift. In the second order in V accuracy, this Lagrangian

signature is partially lost and in higher order in V accuracy this deviation from a nice Lagrangian signature increases. First order in V accuracy Eqn. (50) and the next two can be bunched into

$$\frac{\Delta \nu_{pq}}{\nu_p} = \frac{\Delta L_{pq}}{U_0},$$
(53)

in which we dropped the simplification of $U_0 = 1$ and assumed the Lagrangian to be the classical $L = K - V$.

XI.   EXTENDING THE SCHWARZSCHILD METRICS REACH USING THE FFG CONNECTION.

With the FFG approach based on Special Relativity, the Einstein Equivalence Principle and Newton's gravitational potential, first order correct expressions for the gravitational red shift of stationary clocks and of satellites were derived. The second order FFG frequency shift expressions are discussion points, falsifiable/verifiable predictions. In (de Haas, 2014) the geodesic or de Sitter precession was derived using the same method of a free fall grid. So independent of GR and Schwarzschild, only in the EPS Weyl Space CP-P or FFG environment, curvature effects were correctly derived. Conceptually it was possible to split the end result of the geodesic precession in a Schouten precession part and a Thomas precession part, with the first interpreted as the space-like contribution and the second as the time-like contribution (de Haas, 2014). This implies that the FFG approach covers both space-like curvature effects and time-like curvature effects, thus both the g_{11} and the g_{00} effects of GR-Schwarzschild. During the development of the FFG method, GR-Schwarzschild provided indispensable guidance, for the precession of the previous paper as for this papers frequency shifts.

The connection between the P and the CP geodesics in EPS Weyl space lead to the Schwarzschild frequency shift g_{00} metric parameter. From the FFG resuls, Eqn. (13) and Eqn. (20), together as

$$\frac{\nu_b}{\nu_a} = \frac{\gamma_b}{\gamma_a} = \frac{\sqrt{1 - \frac{v_a}{c^2}}}{\sqrt{1 + \frac{v_b}{c^2}}} = \frac{\sqrt{1 + \frac{2\Phi_a}{c^2}}}{\sqrt{1 + \frac{2\Phi_b}{c^2}}} = \frac{\sqrt{1 - \frac{2GM}{r_a c^2}}}{\sqrt{1 - \frac{2GM}{r_b c^2}}} = \frac{\sqrt{g_{00}^a}}{\sqrt{g_{00}^b}},$$
(54)

we conclude that $\sqrt{g_{00}} = 1/\gamma_\phi$ to first order in ϕ/c^2 series expansion. In this expression, γ_ϕ is determined by the r dependent free fall velocity on the CP geodesic at the location of

the relevant P geodesic. Then also $g_{00} = 1/\gamma_\phi^2$ in the first order to γ_ϕ escape velocity and gravitational energy range. Which suggests that the Schwarzschild metric or solution to the Einstein Equations might not be best suited for second order and higher in Φ/c^2 accuracy.

If the EPS claim, as repeated by (Capozziello et al., 2012), that the Ehlers-Pirani-Schild formalism *provides a natural interpretation of the observables showing how relate them to General Relativity and to a large class of Extended Theories of Gravity* is of any value, then it should be allowed to try to phenomenologically and constructively extend the reach of the Schwarzschild metric based on the P to CP approach. The EPS Weyl space formalism should then be able to translate, or at least relate, the extension of the Schwarzschild metric to Riemann space and eventually to the Einstein Equations. So what I do next is to phenomenologically guess a (stronger field of gravity extension of the) Schwarzschild metric that would fully match with the EPS Weyl Space P-CP environment I have set up in this paper. The leading question is what the form of the Schwarzschild metric had to be if the Schwarzschild result were to match the FFG to higher order of accuracy in Φ/c^2. I have no claims at all regarding the result of the hypothetical exercise, other than that such a form of g_{00} (and coupled g_{11}) would give the same gravitational redshift predictions as the FFG. This result can be compared to the PPN perturbation of g_{00} as for example in (Kopeikin, 2009; Castel-Branco et al., 2014).

With $g_{00} = 1/\gamma_\phi^2$ to first order in ϕ/c^2 series expansion and also $\gamma_\phi = 1 - \Phi/c^2$ to any order, the conditions can be relaxed a little in order to see what happens when the first order restriction on $g_{00} = 1/\gamma_\phi^2$ are dropped. This would give

$$g_{00} = \frac{1}{\gamma_\phi^2} = \frac{1}{\left(1 - \frac{\phi}{c^2}\right)^2} = \frac{1}{\left(1 + \frac{M}{r}\right)^2}, \tag{55}$$

with $G = c = 1$ at the end right hand side. The Taylor series expansion results in

$$g_{00} = \frac{1}{\left(1 + \frac{M}{r}\right)^2} = 1 - \frac{2M}{r} + 3\frac{M^2}{r^2} + \mathcal{O}(\frac{M^3}{r^3}) \tag{56}$$

to get back to the Schwarzschild metric in two steps, starting with the second order as

$$g_{00} = 1 - \frac{2M}{r} + 3\frac{M^2}{r^2} \tag{57}$$

and then to first order as

$$g_{00} = 1 - \frac{2M}{r}. \tag{58}$$

With

$$\sqrt{g_{00}} = \sqrt{1 - \frac{2M}{r} + 3\frac{M^2}{r^2}} \tag{59}$$

constructed this way one would evidentially have equal gravitational redshifts to second order in ϕ/c^2 accuracy.

In (Ruggiero et al., 2008) the Schwarzschild metric is given in polar coordinates as

$$ds^2 = -\left(1 - \frac{2M}{r}\right)dt^2 + \left(1 - \frac{2M}{r}\right)^{-1}dr^2 + r^2(d\theta^2 + sin^2\theta d\phi^2), \tag{60}$$

with the usual $G = c = 1$. Using the above for g_{00} one will get the unlimited field strength extension of the Schwarzschild metric as

$$ds^2 = -\frac{1}{\left(1 + \frac{M}{r}\right)^2}dt^2 + \left(1 + \frac{M}{r}\right)^2 dr^2 + r^2(d\theta^2 + sin^2\theta d\phi^2). \tag{61}$$

I apply the interpretation

$$\left(1 + \frac{M}{r}\right)^2 = \frac{1}{\frac{1}{\left(1 + \frac{M}{r}\right)^2}} \approx \frac{1}{1 - \frac{2M}{r} + 3\frac{M^2}{r^2} + \mathcal{O}(\frac{M^3}{r^3})} \tag{62}$$

to get full symmetry in the series expansion approximation. In the second order in ϕ/c^2 this would result in the metric

$$ds^2 = -\left(1 - \frac{2M}{r} + 3\frac{M^2}{r^2}\right)dt^2 + \left(1 - \frac{2M}{r} + 3\frac{M^2}{r^2}\right)^{-1}dr^2 + r^2(d\theta^2 + sin^2\theta d\phi^2), \tag{63}$$

This will then lead to a second order static redshift that evidently matches our second order redshift. Which was the sole goal of this exercise. When Eqn. (57) is combined with the method behind Eqn. (25), we get

$$g_{00} = 1 - \frac{2M}{r} + 3\beta\frac{M^2}{r^2} \tag{64}$$

with $\beta = 1$ for the FFG based extended SR-Schwarzschild metric.

The big question for the next decades will be if the Schwarzschild metric as exact solution of the Einstein Equations is going to withstand the second order in ϕ/c^2 accuracy tests of the gravitational redshift. If not, will the proposed theoretical results of this paper be verified? Perhaps the PPN formalism, smartly extending the reach of the Schwarzschild metric by perturbation methods as in (Kopeikin, 2009; Castel-Branco et al., 2014), will produce the correct results.

XII. CONCLUSION

Given the future task of designing GNSS 2.0 in the 0.1 mm accuracy range, some competition among the fundamental theorists couldn't hurt. If all fundamental theoretical research in this area is to be in the GR-Schwarzschild paradigm or not to be and the attempts to integrate a robust GNSS into this paradigm fail, then you have a problem. It might even be that future GNSS second order tests prove the GR-Schwarzschild predictions to be inadequate for second order accuracy,

The alternative PPN approach, although highly flexible and with an excellent performance track, isn't fundamental by itself. PPN is designed to adapt to any fundamental (=metric) theory of gravity. It can only become accurate itself after enough measurements are available to fix the PPN parameters to useful values, so after a test-version of GNSS 2.0 is operational.

It is my opinion that the pragmatic version of the EPS Weyl Space approach, as developed in this paper in a Minkowski-EEP environment, might be an intermediate stage in the fundamental research efforts towards GNSS 2.0. The advantage of my approach is that it works with an easily imaginable global grid of free fall clocks instead of a highly abstract global curved metric as its background. The conceptual language used to present the global grid approach is highly compatible with the language of today's GNSS 1.0.

The FFG approach is not an alternative but an intermediate theory of gravity, as are all Minkwoski-EEP approaches. The motivation behind most of the Minkowski-EEP investigations is to produce conceptual anchor points and arguments for a subsequent or a forgoing (as is usually the case) fully curved metric theory of gravity. The EPS Weyl space analysis might provide a link between the FFG approach and GR.

As for alternative theories of gravity, as for example the f(R) theories as explored in the already cited (Castel-Branco et al., 2014), I couldn't find alternative approaches towards a relativistic GNSS design in first order accuracy, so let alone in the second order accuracy range.

REFERENCES

Ashby, N. (2002, May). Relativity and the global positioning system. *Physics Today 55*(5), 41–47.

Ashby, N. (2003, Jan). Relativity in the global positioning system. *Living Reviews in Relativity 6*(1).

Ashby, N. (2006). Relativistic effects in the global positioning system. Accessed online 2017.

Ashby, N., Heavner, T. P., Jefferts, S. R., Parker, T. E., Radnaev, A. G., and Dudin, Y. O. (2007, Feb). Testing local position invariance with four cesium-fountain primary frequency standards and four nist hydrogen masers. *Phys. Rev. Lett. 98*, 070802.

Bahder, T. B. (2001). Navigation in curved space-time. *American Journal of Physics 69*(3), 315–321.

Bahder, T. B. (2003, Sep). Relativity of gps measurement. *Phys. Rev. D 68*, 063005.

Bertolami, O. and J. Páramos (2011). Using global positioning systems to test extensions of general relativity. *International Journal of Modern Physics D 20*(09), 1617–1641.

Blanchet, L., Salomon, C., Teyssandier, P., and Wolf, P. (2001). Relativistic theory for time and frequency transfer to order c^{-3}. *A&A 370*(1), 320–329. ArXiv: 0010108 [gr-qc].

Čadež, A., U. Kostić, P. Delva, and S. Carloni (2011). Mapping the spacetime metric with a global navigation satellite system-extension study: Recovery of orbital constants using intersatellite links. *European Space Agency, the Advanced Concepts Team*. European Space Agency, the Advanced Concepts Team, Ariadna
nal report (09/1301 ccn). Technical report.

Capozziello, S., M. De Laurentis, L. Fatibene, and M. Francaviglia (2012). The physical foundations for the geometric structure of relativistic theories of gravitation. from general relativity to extended theories of gravity through ehlers-pirani-schild approach. *International Journal of Geometric Methods in Modern Physics 09*(08), 1250072. arXiv:1202.5699 [gr-qc].

Carrol, S. M. (2004). *Spacetime and Geometry. An Introduction to General Relativity.* San Francisco: Addison Wesley.

Castel-Branco, N., J. Pramos, and R. March (2014). Perturbation of the metric around a spherical body from a nonminimal coupling between matter and curvature. *Physics Letters B 735*(Supplement C), 25 – 32.

Chou, C. W., D. B. Hume, T. Rosenband, and D. J. Wineland (2010). Optical clocks and relativity. *Science 329*(5999), 1630–1633.

Coll, B. (2001). Physical relativistic frames. In *Journées 2002: Systèmes de Référence Spatio-Temporels, Brussels, Belgium, 24-26 September 2001*.

Coll, B. (2003). A principal positioning system for the earth. In *Journees 2002: Space and Time References Systems: Astrometry from Ground and from Space (JSR 2002) Bucharest, Romania, September 25-28, 2002.* arXiv:0306043 [gr-qc].

Coll, B. (2013). relativistic positioning systems: Perspectives and prospects. In *Workshop on Relativistic Positioning Systems and their Scientific Applications Brdo, Slovenia, September 19-21, 2012.* arXiv:1302.5782 [gr-qc].

de Haas, E. P. J. (2014). The geodetic precession as a 3d schouten precession and a gravitational thomas precession. *Canadian Journal of Physics 92*(10), 1082–1093.

Delva, P. and J. Lodewyck (2013). Atomic clocks: new prospects in metrology and geodesy. In *Workshop on Relativistic Positioning Systems and their Scientific Applications Brdo, Slovenia, September 19-21, 2012.* arXiv:1308.6766 [physics.atom-ph].

Ehlers, J., F. A. E. Pirani, and A. Schild (2012). Republication of: The geometry of free fall and light propagation. *General Relativity and Gravitation 44*(6), 1587–1609. Original paper: J. Ehlers, F. A. E. Pirani and A. Schild, in: General Relativity, papers in honour of J. L. Synge. Edited by L. OReifeartaigh. Oxford, Clarendon Press 1972, pp. 6384.

Einstein, A. (1907). Über das relativitätsprinzip und die aus demselben gezogenen folgerungen. *Jahrbuch cler Raclioaktivitiit uncl Elektronik 4*, 411–462.

Einstein, A. (1916). Über friedrich kottlers abhandlung "über einsteins äquivalenzhypothese und die gravitation". *Annalen der Physik 51*, 639–642.

ESA (2010). Improving the accuracy of satellite navigation systems. ESA Advanced Concepts Team, Accessed online 2015.

Gomboc, A., M. Horvat, and U. Kostić (2014). Relativistic global navigation system. *European Space Agency, PECS*. UL-FMF Reference No. ESA-Gomboc-2014-Final Report.

Hećimović, Ž. (2013). Relativistic effects on satellite navigation. *Tehnički vjesnik 20*(1), 195–203.

HESS Collaboration (2016). Acceleration of petaelectronvolt protons in the galactic centre. *Nature 531*(7595), 476–478. arXiv:1603.07730 [astro-ph.HE].

Jaffe, J. and R. F. C. Vessot (1973). The second order gravitational redshift. *NASA*. Grant

NCR 09-015-205.

Jaffe, J. and R. F. C. Vessot (1976). Feasibility of a second-order gravitational red-shift experiment. *Phys. Rev. D 14*, 3294–3300.

Kheyfets, A. (1991). Spacetime geodesy. *American Journal of Physics*. Weapons Laboratory, Air Force Systems Command, Kirtland Air Force Base, New Mexico, Technical Report No. WL-TN-90-13.

Kopeikin, S. M. (2009). Post-newtonian limitations on measurement of the ppn parameters caused by motion of gravitating bodies. *Monthly Notices of the Royal Astronomical Society 399*(3), 1539–1552. ArXiv:0809.3433 [gr-qc].

Kopeikin, S. M., I. Y. Vlasov, and W. B. Han (2017). The normal gravity field in relativistic geodesy. *ArXiv e-prints*. arXiv:1708.09456 [gr-qc].

Kostić, U., M. Horvat, and A. Gomboc (2015). Relativistic positioning system in perturbed spacetime. *Classical and Quantum Gravity 32*(21), 215004. arXiv:1510.04457 [gr-qc].

Mayrhofer, R. and R. Pail (2012). Future satellite gravity field missions: Feasibility study of post-newtonian method. In S. Kenyon (Ed.), *Geodesy for Planet Earth*, Volume 136 of *International Association of Geodesy Symposia*, pp. 231–238. Springer International Publishing. Switzerland.

Nobili, A. M., D. M. Lucchesi, M. T. Crosta, M. Shao, S. G. Turyshev, R. Peron, G. Catastini, A. Anselmi, and G. Zavattini (2013). On the universality of free fall, the equivalence principle, and the gravitational redshift. *American Journal of Physics 81*, 527–536.

Norton, J. D. (1985). What was einstein's principle of equivalence? *Studies in History and Philosophy of Science 16*, 203–246.

Ohanian, H. and R. Ruffini (2013). *Gravitation and Spacetime* (3 ed.). New York: Cambridge University Press.

Pascual-Sánchez, J., A. Miguel, and F. Vicente (2013). Relativistic versus newtonian frames. *Positioning 4*, 109–114.

Perlick, V. (2016). Using clocks for probing the geometry of spacetime. In *309th Heraeus Seminar "Relativistic Geodesy", Bad Honnef, Germany, 14-18 March 2016*. Slides accessed 2017.

Pound, R. V. and Rebka, G. A. Jr. (1960). apparent weight of photons. *Phys. Rev. Lett. 4*, 337–341.

Puchades, N. and D. Sáez (2015). Relativistic positioning in schwarzschild space-time. *J.*

Phys.: Conf. Ser. 600, 012054. Spanish Relativity Meeting (ERE 2014): almost 100 years after Einstein's revolution.

Puchades, N. and D. Sáez (2016). Approaches to relativistic positioning around earth and error estimations. *Advances in Space Research 57*(1), 499 – 508.

Rindler, W. (2001). *Relativity. Special, General and Cosmological.* New York: Oxford University Press.

Rohrlich, F. (1963). The principle of equivalence. *Annals of Physics 22*, 169–191.

Ruggiero, M. L., D. Bini, A. Geralico, and A. Tartaglia (2008). Emission versus fermi co-ordinates: applications to relativistic positioning systems. *Classical and Quantum Gravity 25*(20), 205011. arXiv:0809.0998 [gr-qc].

Seibert, G. and B. Fitton (2001). Introduction. In B. Fitton and B. Battrick (Eds.), *A world without gravity*, pp. 5–34. Noordwijk: ESA.

The Pierre Auger Collaboration (2017). Observation of a large-scale anisotropy in the arrival directions of cosmic rays above $8 \cdot 10^{18}$ ev. *Science 357*(6357), 1266–1270.

Thoudam, S., Rachen, J. P., van Vliet, A., Achterberg, A., Buitink, S., Falcke, H., and Hran-del, J. R. (2016). Cosmic-ray energy spectrum and composition up to the ankle: the case for a second galactic component. *Astronomy & Astrophysics 595*, A33. arXiv:1605.03111 [astro-ph.HE].

Turneaure, J. P., C. M. Will, B. F. Farrell, E. M. Mattison, and R. F. C. Vessot (1983, Apr). Test of the principle of equivalence by a null gravitational red-shift experiment. *Phys. Rev. D 27*, 1705–1714.

Varičak, V. (1912). Über die nichteuklidische interpretation der relativtheorie. *Jahresbericht der Deutschen Mathematiker-Vereinigung 21*, 103–127.

Will, C. M. (2010). Resource letter ptg-1: Precision tests of gravity. *American Journal of Physics 78*(12), 1240. arXiv:1008.0296v1 [gr-qc].

Will, C. M. (2014). The confrontation between general relativity and experiment. *Living Reviews in Relativity 17*(4). Link accessed on 12-20-2014; Update of lrr-2006-3.

Wolf, P., P. Delva, and A. Hees (2017). Clocks in space for tests of fundamental physics. *Space Science Reviews*.

Xie, Y. (2016). Relativistic time transfer for inter-satellite links. *Frontiers in Astronomy and Space Sciences 3*, 15.